Fractionation and Characterization of a 1-Butene Linear Low Density Polyethylene*

H. SPRINGER, A. HENGSE, and G. HINRICHSEN, *Technical University of Berlin, Institute of Nonmetallic Materials, Polymer Physics, Englische Str. 20, D-1000 Berlin 12, FRG*

Synopsis

A commercial 1-butene LLDPE, Stamylex 1048, is cross fractionated by dynamic direct extraction and subsequent solution crystallization. The fractions are characterized by determining molecular masses M_η, M_n, and M_w and the comonomer content. DTA measurements are performed on unannealed and annealed samples of the fractions. The temperatures and specific heats of crystallization and fusion can be interpreted by reflecting the influence of molecular weight and comonomer content. The presented results are compared to data of 1-butene LLDPE published in the recent literature.

INTRODUCTION

Linear low density polyethylene (LLDPE) exhibits some superior qualities in comparison to conventional low density polyethylene (LDPE): greater tensile and tear strength as well as higher environmental stress crack resistance.[1,2] This leads to better economy of this material, higher ductility, and enhanced operating reliability. Great effort has been undertaken to understand these phenomena by the particular chemical structure of LLDPE. Thus, fractionation and characterization of LLDPE have found growing interest in the recent literature. As one important result, the complex melting behaviour of LLDPE could be attributed to intermolecular variation of comonomer content.[3-8]

Various fractionation methods (successive solution fractionation,[7] solvent extraction,[9,10] dynamic direct extraction,[3,5,11] solution crystallization,[9,12,13] temperature rising elution fractionation,[4,5,7,8,14-17] and solvent gradient elution fractionation[18] as well as combined methods of these[4,5,7,9,18] have been applied to obtain fractions differing in molecular weight and comonomer content. The fractions and the unfractionated LLDPE have been characterized according to molecular weight and molecular weight distribution by viscosity measurements[4,5,8,11,13,16] or gel permeation chromatography.[4,5,7-12,15-18,23,24] The comonomer content has been measured by infrared absorption[4,5,7,9,14,16,18,19,25] and/or NMR spectroscopy.[6,8,9,10,17,19-24] In some cases also the comonomer statistics have been investigated by the latter method.[10,18,21,22] Analytical temperature rising elution fractionation has been used after calibration to observe the mass distribution of comonomer content.[7,16,21,23]

* Dedicated to Prof. Dr. E. W. Fischer on the occasion of his 60th birthday.

Journal of Applied Polymer Science, Vol. 40, 2173-2188 (1990)
 CCC 0021-8995/90/11-122173-16$04.00

In general, interdependences between comonomer content and other physical properties (e.g., crystallization temperature, crystallinity, and melting point) have been established, showing similar tendencies throughout the literature. But with respect to quantitative agreement significant differences appear. The main reason for these apparent discrepancies is the existence of other parameters than comonomer content which also influence the corresponding physical properties. The most important additional parameters are molecular mass, comonomer statistic and sample preparation. Moreover, measuring conditions must be taken into consideration.

This article deals with cross fractionation and characterization of a commercial 1-butene ethylene copolymer and its fractions and intends to illustrate the influence of parameters other than comonomer content on melting point and heat of fusion.

EXPERIMENTAL

Material

A linear low density polyethylene, Stamylex 1048 (DSM), a 1-butene ethylene copolymer, was used. An investigation on crystallization and melting behaviour of this material has been reported in Ref. 26.

Fractionation

Two different fractionation methods were applied in order to obtain fractions varying in molecular weight and in comonomer content. In a first step successive solution fractionation was carried out by dynamic direct extraction according to Ref. 11 in order to receive narrow molecular weight distribution fractions. In a second step the fraction of greatest mass percentage (fraction S6a) was fractionated by solution crystallization which subdivides this fraction according to the comonomer content.

Direct extraction was performed using *p*-xylene as solvent and ethylene glycol mono etyl ether (EGME) as nonsolvent. Mixtures increasing from 42 to 66% xylene at 4% steps were used. Extraction temperature was 125°C and 2,6-di-tert-butyl-4-methyl phenol was chosen as stabilizer.

Solution crystallization was carried out in pure xylene at 80, 65, 50, and 23°C. The initial concentration was 8 g/L, and the crystallization period took 6 h.

Characterization Methods

Molecular Weight

The viscosity average molecular weight M_η was measured solving 2–4 g/L LLDPE in decahydronaphthalene at 135°C in an Ostwald viscosimeter. For evaluating M_η values from the extrapolated intrinsic viscosities the following Mark–Houwink constants were chosen: $K_{[\eta]} = 62$ mL/kg and $a = 0.70$.[27] GPC measurements were made using a Knauer high temperature equipment with o-dichlorobenzene (ODCB) as eluent. The column was filled with highly crosslinked spherical polystyrene/divinylbenzene particles of 10 μm diameter and

pore sizes ranging from 50 to 10^5 nm. Elution temperature was 145°C and elution rate 0.5 mL/min. A RI-detector was used. Average molecular weights M_n and M_w were calculated using a calibration curve of linear PE standards.

Comonomer Content

As an index of comonomer content (more exactly: CH_3 content) the ratio of the IR absorbancies of the 1378 and 1368 cm^{-1} bands was determined. The 1378 cm^{-1} band is attributed to a symmetrical deformation vibration $\delta_s(CH_3)$ of the methyl group and the 1368 cm^{-1} band to a wagging vibration $\gamma_w(CH_2)$ of the methylene group.[9,19,28] Unfortunately both bands overlap and moreover there exist further overlapping CH_2 vibrations.[9,29,30] Nevertheless, the above mentioned ratio is shown to be a good measure of comonomer content.

A quantitative method of evaluating the IR spectrum consists of subtracting from the LLDPE spectra a spectrum of a highly linear PE, being nearly free of CH_3 groups, and of evaluating the remaining peak of the difference spectrum at 1378 cm^{-1}.[9,19] The number N_{1000C} of ethyl branches per 1000 C atoms was determined according to Ref. 19 by

$$N_{1000C} = KA/(d \cdot \rho) \tag{1}$$

with K being the reciprocal extinction coefficient (K = 0.59 g/cm^2), A the absorbance, d the thickness and ρ the density of the measured sample. The reference spectrum was taken from a high molecular weight linear PE (Hostalen GUR from Hoechst). Because of difficulties in measuring the thickness d and density ρ of all the samples with the necessary precision, the term $d \cdot \rho$ was calculated from the factor ξ, by which the intensities of the reference spectrum have to be multiplied, according to

$$d \cdot \rho = d_r \rho_r \xi \tag{2}$$

where d_r and ρ_r are the thickness and the density of the reference sample. In doing this, it was supposed that the absorbance of the IR peaks used for compensation are not influenced by variation of crystallinity or ethyl content. The IR spectra were measured on a FTIR spectrometer (10 DX, Nicolet).

The most reliable method of evaluating the comonomer statistic is ^{13}C-NMR spectroscopy.[9,17,19] Therefore a few selected samples were additionally characterized by this method. The spectra were recorded on a Varian XL 200 NMR spectrometer operating at 50.1 MHz. Instrumental conditions were as follows: pulse angle 45°, spectral width 10 kHz, number of data points per spectrum 20,000. Polymer solutions were prepared in deuterated ODCB with a concentration of about 2 g/100 mL. Measurements were performed at 100°C with broad band decoupling. Intensities were evaluated from integrated areas. From the spectra the investigated LLDPE was identified as ethylene 1-butene copolymer. The comonomer content thus was calculated according to Ref. 19

$$\epsilon_z = I_\beta/(7I_\beta + 2I_m) \tag{3}$$

where ϵ_z is the number of ethyl groups divided by the total number of carbon

atoms. I_β and I_m are the integral intensities of the β-C-atom and of the main peak of backbone atoms, respectively. From Eq. (1) and (3) one obviously gets

$$N_{1000C} = 1000\epsilon_z \tag{4}$$

Crystallization and Melting Behavior

DTA Measurements

Melting and crystallization curves were recorded on a Mettler TA 2000. 5–10 mg of a sample were weighed into a DTA pan. To eliminate thermal history, samples were first heated up to 443 K and subsequently kept at this temperature for 10 minutes. Then they were cooled down to 233 K with a rate of 10 K/min and the recorded DTA traces are shortly called "crystallization curves." Thereafter "melting curves" were measured heating the samples from 233 K to 443 K with a rate of 10 K/min. Further, melting curves of samples annealed at 373 K for 24 h were recorded under the same conditions.

Density Measurements

Density was measured using a density gradient column filled with mixtures of *i*-propanol and water.

RESULTS

Molecular Masses

Tables I and II summarize the molecular masses M_η, M_n, and M_w and the mass percentage of the various fractions of the direct extraction of the whole polymer and solution crystallization of fraction 6a, respectively. Fractions 6 and 7 could be divided into a powdery and a more compact subfraction, denoted by a and b, respectively. The molecular weight distribution curves, as seen from the RI-elution volume diagrams of GPC, show only one maximum.

TABLE I
Direct Extraction: Fractionation Data and Molecular Weights

Fraction number	Volume fraction of *p*-xylene (%)	Mass fraction (%)	M_η (g/mol)	M_n (g/mol)	M_w (g/mol)	M_w/M_n
S1	42	7.1	3700	4600	7500	1.63
S2	46	2.1	5600	7000	9600	1.37
S3	50	3.7	11,300	10,700	15,200	1.42
S4	54	9.3	16,300	16,300	22,400	1.37
S5	58	13.2	24,300	25,200	34,300	1.36
S6a	62	24.5	63,100	37,100	68,800	1.85
S6b	62	7.7	68,300	46,500	83,800	1.80
S7a	66	11.2	87,700	43,200	93,500	2.16
S7b	66	11.4	128,000	49,300	144,500	2.93
Whole polymer Stamylex 1048	—	—	42,000	26,200	91,800	3.50

TABLE II
Solution Crystallization of Fraction S6a: Fractionation Data and Molecular Weights

Fraction number	Crystallization temperature (°C)	Mass fraction (%)	M_η (g/mol)	M_n (g/mol)	M_w (g/mol)	M_w/M_n
S6-80	80	20.2	62800	41000	69700	1.70
S6-65	65	28.0	50800	39900	70400	1.76
S6-50	50	19.5	51600	31800	62200	1.96
S6-23	23	14.2	56500	—	—	—
S6a	—	—	63100	37100	68800	1.85

Comonomer Content

The ratio A_{1378}/A_{1368} of the absorbances at 1378 cm^{-1} and 1368 cm^{-1} and the numbers N_{1000C} evaluated from the IR difference spectrum (Eq. (1)) and from ^{13}C-NMR (Eq. (3)) are listed in Table III.

DTA Measurement

The crystallization and melting curves of unannealed samples and the melting curves of annealed samples are represented in Figures 1 and 2. Scale bars together with the factor at the right end of each DTA curve indicate the scale of the corresponding curve. For example, in Figure 1(a) the ordinate scale represents a value of 4.9 $Jg^{-1}K^{-1}$ for fraction S7b. Specific heats of fusion and crystallization as well as melting and crystallization peak temperatures are listed in Table IV.

Density Measurements

The densities of unannealed and annealed samples (ρ and ρ_a) are given in Table IV.

TABLE III
Comonomer Content

Fraction number	A_{1378}/A_{1368}	N_{1000C} (IR) (from Eq. (1))	N_{1000C} (NMR) (from Eq. (3))
S1	1.59	25.4	25.2
S2	1.48	23.0	22.8
S3	1.37	21.3	—
S4	1.26	19.2	—
S5	1.13	16.1	20.0
S6a	0.99	13.6	16.1
S6b	0.92	12.6	17.2
S7a	0.93	12.7	16.4
S7b	0.76	10.1	—
Stamylex 1048	1.07	15.0	15.9
S6-23	1.32	19.4	—
S6-50	1.03	14.3	—
S6-65	0.81	10.9	—
S6-80	0.70	9.0	—

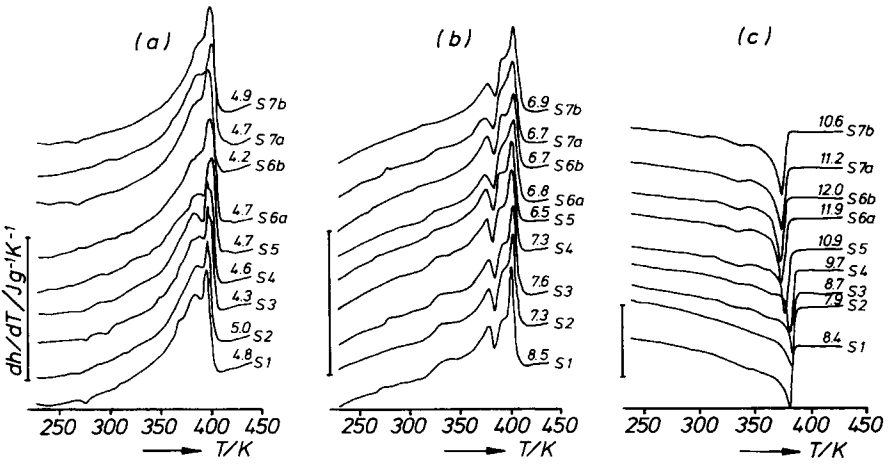

Fig. 1. DTA curves of direct extraction fractions: (a), (b) melting curves of unannealed and annealed samples respectively; (c) crystallization curves. Vertical scale bars together with the factor at the right end of each DTA curve indicate the ordinate scale of the corresponding curve.

DISCUSSION

Fractionation and Characterization

Table I indicates that the direct extraction process yields fractions differing in molecular weights and having polymolecularities from 1.4 to 2.9. The unfractionated sample, Stamylex 1048, has M_w = 91800 g/mol and M_w/M_n = 3.5. About 55% of the mass is concentrated in the two fractions S6 and S7. As can be seen from Table I, the relation $M_n \leq M_\eta \leq M_w$ is not always fullfilled. This may be caused by using improper Mark–Houwink coefficients or by insufficient sensitivity of the RI-detector at low concentrations.[31–33] The molecular masses of the solution crystallized fractions do not show any systematic variation with crystallization temperature. The relationship between the logarithm of the vis-

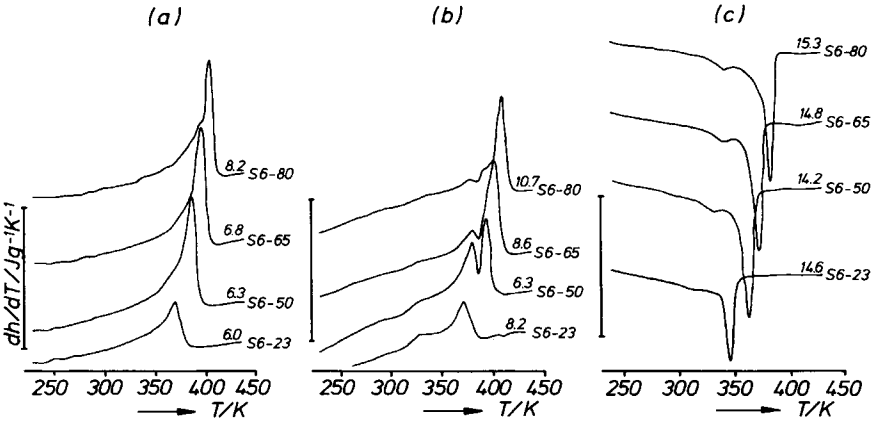

Fig. 2. DTA curves of solution crystallized fractions: a, b and c as well as the scale bars and factors at the right curve ends have the same meaning as in Figure 1.

TABLE IV
Densities, Peak Temperatures and Specific Heats of Fusion and Crystallization

Fraction number	T_c (K)	T_m (K)	T_{ma} (K)	Δh_c (J/g)	Δh_f (J/g)	Δh_{fa} (J/g)	ρ (g/cm^3)	ρ_a (g/cm^3)
S1	379	394	400	114	132	150	0.924	0.929
S2	380	395	402	110	142	143	0.926	0.929
S3	381	396	402	106	116	146	0.927	0.926
S4	379.5	396	401	90	118	146	0.916	0.924
S5	375	399	401	91	120	117	0.918	0.922
S6a	370.5	397	403	105	122	138	0.917	0.919
S6b	371	396	403	96	102	115	0.919	0.917
S7a	371.5	399	402	98	126	130	0.917	0.918
S7b	366.5	397	403	98	114	122	0.916	0.922
Stamylex 1048	374	397	400	114	124	126	—	—
S6-23	344	369	373	59	73	65	0.918	0.910
S6-50	361	385	394	89	118	109	0.915	0.916
S6-65	370	394	403	107	128	142	0.922	0.923
S6-80	382	403	408	102	145	159	0.935	0.937

[a] The indices of T, Δh and ρ mean: a—annealed sample, c—crystallization, m—melting, f—fusion.

cosity average molecular weight M_η and the volume fraction of xylene ϕ_x can be approximated by two straight lines. This was also found for data taken from Ref. 11, where a high density polyethylene was extracted at 122°C (Fig. 3). The molecular weight at the break point is about 30,000 g/mol. Thus the following empirical relation may be written down:

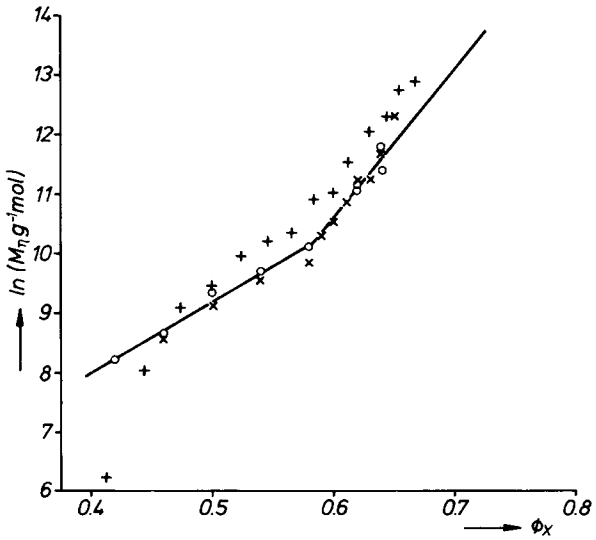

Fig. 3. Logarithm of M_η as a function of solvent fraction ϕ_x: (○) data of the present work; (×) data according to Refs. 11; (+) data according to Ref. 18.

$$M_\eta = A \exp(B\phi_x)$$

where $A = 2.75$ g/mol and $B = 11.8$ for $M_\eta \leq 30000$ g/mol

and $A = 0.0134$ g/mol and $B = 24.8$ for $M_\eta \geq 30000$ g/mol (5)

The fractions of direct extraction do not only differ in molecular weight but also in ethyl content. In Figure 4 the ratio A_{1378}/A_{1368} and N_{1000C} are plotted against volume fraction ϕ_x of xylene. Neglecting the subfractions 6b and 7b, linear relationships are found

$$A_{1378}/A_{1368} = 2.75 - 2.8\phi_x \tag{6a}$$

and

$$N_{1000C} = 48.9 - 55.9\phi_x \tag{6b}$$

Clearly, this result cannot be attributed to methyl groups at the ends of the main chains. For, firstly this effect would be expected to be much weaker and moreover there are also vinyl end groups as can be recognized from the IR spectra. Figure 5 represents the interdependence between A_{1378}/A_{1368} and N_{1000C}

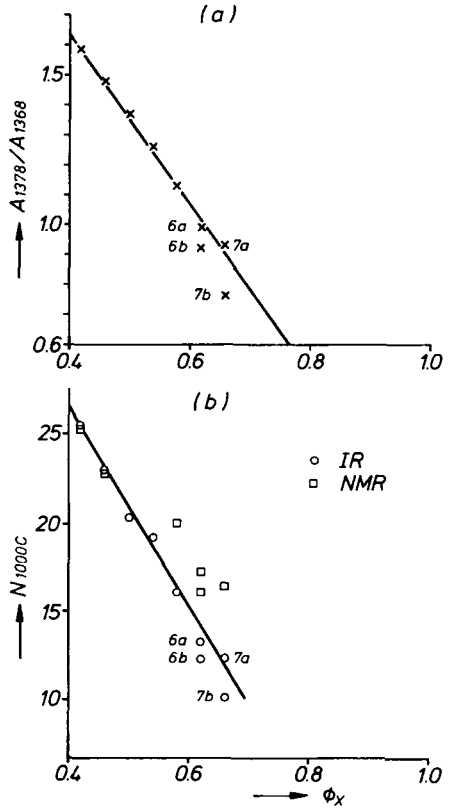

Fig. 4. The ratio A_{1378}/A_{1368} (a) and N_{1000C} (b) as a function of solvent fraction ϕ_x.

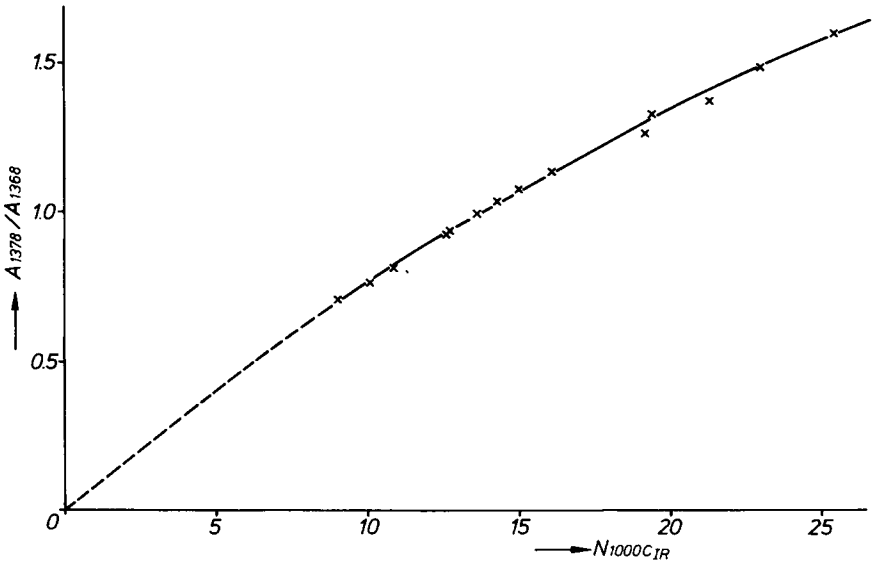

Fig. 5. The ratio A_{1378}/A_{1368} versus N_{1000C} as determined by IR measurements.

calculated according to Eq. (1). A good correlation can be established, not very surprising, because both quantities are taken from the same IR spectra. The systematic deviation from proportionality indicates the problems, which arise when the ethyl content is determined by IR measurements alone without controlling variations of morphology.

From Figure 6 the following linear relation between N_{1000C} and ln M_η can be derived

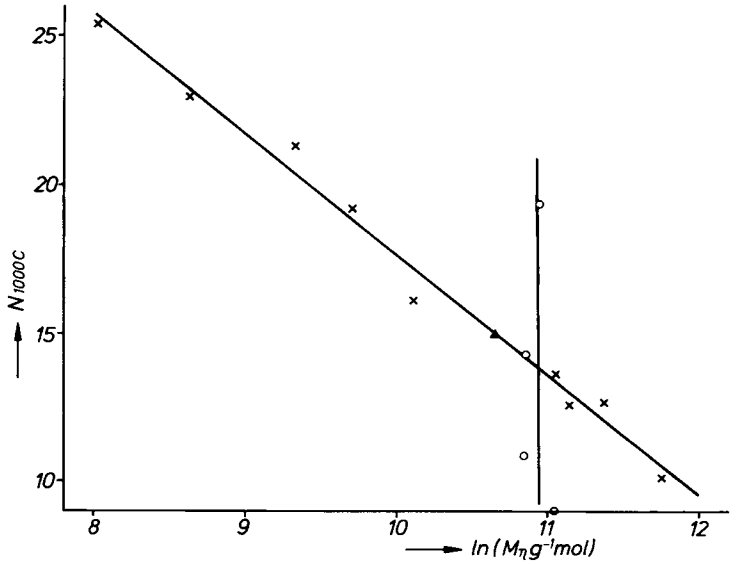

Fig. 6. N_{1000C} versus logarithm of M_η for samples of direct extraction (×) and of solution crystallization (○) and Stamylex 1048 (▲).

$$N_{1000C} = 58.1 - 4.05 \ln(M_\eta \cdot g^{-1} \cdot mol) \quad (7)$$

Similar linear relationships can be found from Figures 6 and 7 of (4)

$$N_{1000C} = 86 - 6.05 \ln(M_\eta \cdot g^{-1} \cdot mol) \quad (8a)$$

for gas phase 1-butene LLDPE, and

$$N_{1000C} = 49.7 - 2.78 \ln(M_\eta \cdot g^{-1} \cdot mol) \quad (8b)$$

for a high pressure 1-butene LLDPE. Thus, the correlation between N_{1000C} and ln M_η can be described by the same type of function ($N_{1000C} = A - B \ln(M_\eta \cdot g^{-1} \cdot mol)$) while the constants A and B depend on the particular polymerization conditions for the different 1-butene LLDPEs.

The fractionation by solution crystallization is mainly controlled by differences in the comonomer content between the molecules of the same fraction of direct extraction. The molecular weight plays a minor role (cf. Table II). Figures 7a and 7b show the dependence of A_{1378}/A_{1368} and N_{1000C} respectively on the crystallization temperature T_c. Again linear relationships can be derived. The equation

$$N_{1000C} = 23.6 - 0.186 T_c/°C \quad (9)$$

may be compared with data given in (9) for an ethylene 1-butene copolymer prepared by Ziegler type polymerization which yield also a linear relationship

$$N_{1000C} = 20 - 0.22 T_c/°C \quad (10)$$

As before, we get the same type of equation, but the constants differ. This result may be explained in the same way as above.

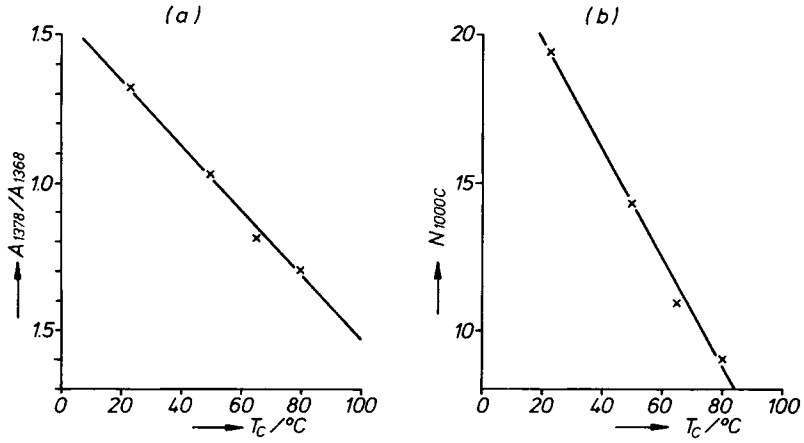

Fig. 7. The ratio A_{1378}/A_{1368} (a) and N_{1000C} (b) as a function of crystallization temperature T_c.

Melting and Crystallization

The melting and crystallization behavior of the various fractions is influenced by both molecular mass and ethyl content.

The DTA curves of the direct extraction fractions exhibit a broad melting and crystallization region (Fig. 1). Annealing at 373 K produces segregation of material crystallizing at temperatures below the annealing temperature and leads to samples showing multiple melting peaks in the thermograms.

In Figure 8 the temperature of the highest melting peak (T_m, T_{ma}) and of the crystallization peak (T_c) of direct extraction fractions are plotted against molecular weight. The small increase of melting point with increasing M_η can be attributed to the corresponding decrease of comonomer content, while the decrease of crystallization temperature with increasing M_η is due to the fact that segmental mobility decreases with growing chain length.

The melting and crystallization peaks of the solution crystallization fractions (Fig. 2) are narrower than those obtained from fractions of direct extraction. Annealing also induces segregation effects. As is obvious from Figure 9, melting and crystallization temperatures drop with increasing comonomer content.

Similar relationships between melting point and comonomer content for ethylene 1-butene copolymers have been published by several authors.[8,9,17,18,23,24,34,35] For comparison their data are compiled into a common diagram (Fig. 10). Obviously the data scatter within a wide range. The main reason for this variation is: the melting point depends additionally on annealing, molecular weight and comonomer statistics. The annealing effect is clearly seen in Fig. 9 and from the curves 7 and 7′. The difference of the curves 3a and 3b and of 8a and 8b is explained in Refs. 17, 18 by a higher degree of blockness of the comonomer distribution of the samples corresponding to the curves 3b and 8b. The approximate constancy of T_m-values of the direct extraction fractions (Fig. 8) in spite of the comonomer content variation (Fig. 6) is due to

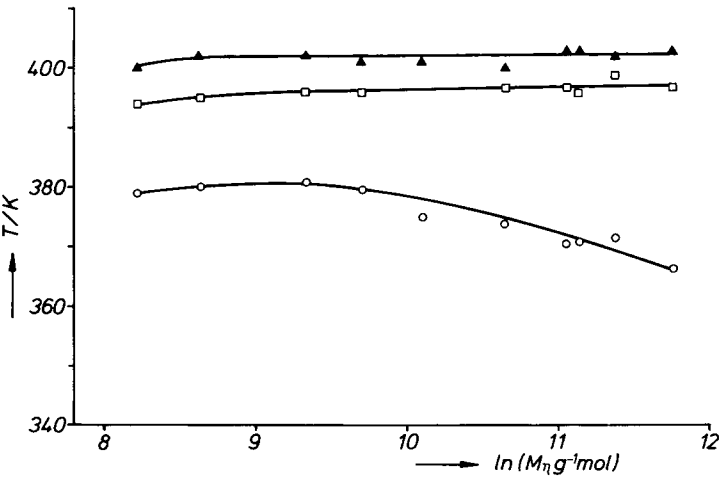

Fig. 8. Melting ((□) unannealed, (▲) annealed samples) and crystallization (○) temperatures of direct extraction fractions versus logarithm of M_η. All temperatures (T_m, T_{ma}, and T_c) are peak temperatures.

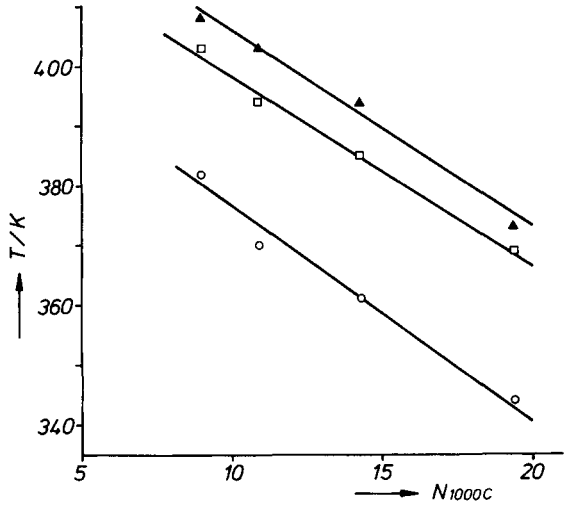

Fig. 9. Melting ((□) unannealed, (▲) annealed samples) and crystallization (○) temperatures of solution crystallized fractions versus N_{1000C}. All temperatures (T_m, T_{ma}, and T_c) are peak temperatures.

the broadness of comonomer distribution within a single fraction. A high degree of blockness also may be the reason for the high values of curves 7 and 7'. The molecular weight dependence can play in Figure 10 only a secondary role, because M_w for nearly all the samples lies within the relatively insensitive range from 50,000 to 200,000 g/mol. Summing up the above discussion the following

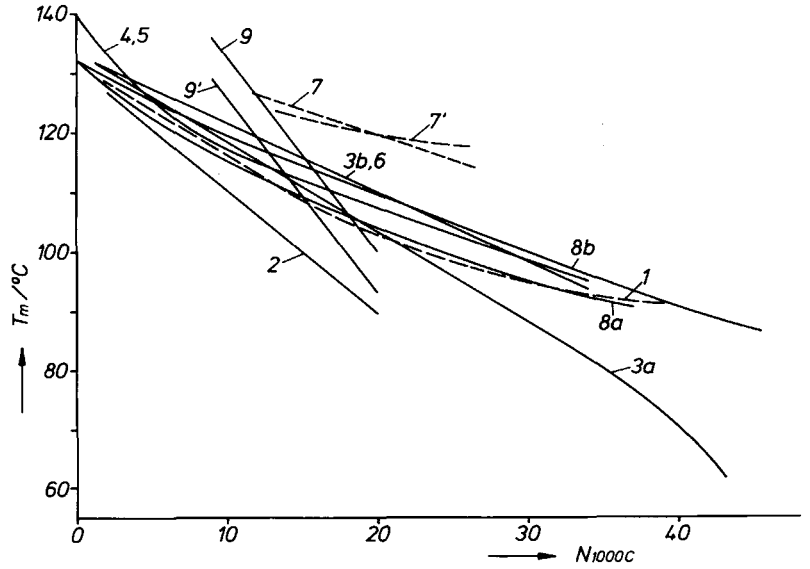

Fig. 10. Relationships between melting points and comonomer content for 1-butene LLDPEs as published in some recent articles. (1, Ref. 8; 2, Ref. 9; 3a, 3b, Ref. 18; 4, Ref. 23; 5, Ref. 24; 6, Ref. 34; 7, 7', Ref. 35; 8a, 8b, Ref. 17); 9, 9', present work.)

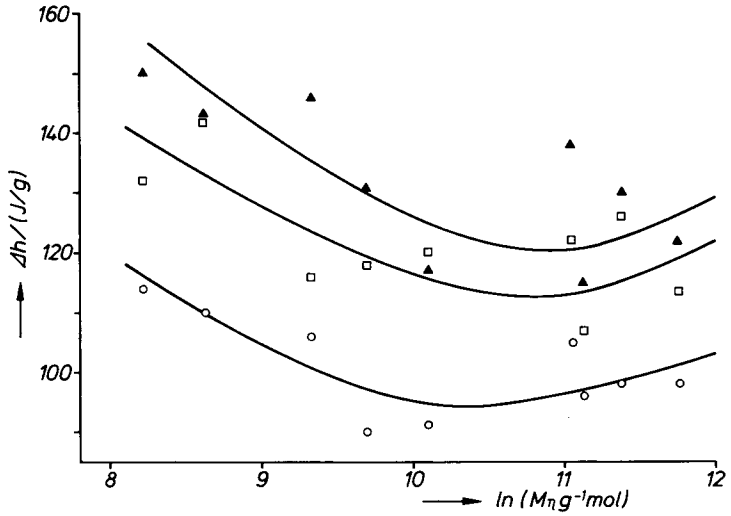

Fig. 11. Heats of fusion ((□) unannealed, (▲) annealed samples) and crystallization (○) of direct extraction fractions as a function of logarithm of M_η.

tendency may be stated: T_m decreases with increasing N_{1000C} the more the narrower the comonomer distribution and the greater the degree of blockness is. Annealing not far below the melting temperature raises the T_m-values.

The course of the heats of fusion and crystallization of the direct extraction fractions as a function of the molecular weight (Fig. 11) can be explained by concurring effects between molecular weight and comonomer content: at low molecular weight the greater chain mobility facilitates crystallization, at high molecular weight crystallization is supported by the lower comonomer content. This phenomenon has been also observed and theoretically deduced in (18).

Keeping the molecular weight constant, the influence of comonomer content on the heat of fusion can be isolated. As seen from Figure 12 the heat of crys-

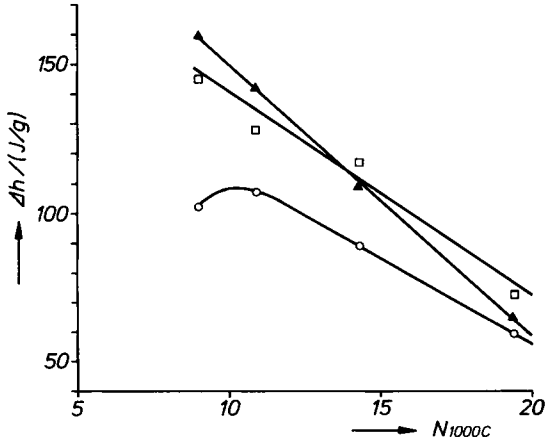

Fig. 12. Heats of fusion ((□) unannealed, (▲) annealed samples) and crystallization (○) of solution crystallized fractions as a function of N_{1000C}.

tallization and fusion decreases with increasing comonomer content. In Figure 13 similar relationships of ethylene 1-butene copolymers, found in some recent publications on LLDPE, are compared with the present work. All curves show the same tendency: Δh_f decreases with increasing comonomer content, N_{1000C}. But the absolute values spread over a wide range. This may be caused by several reasons:

1. Systematic errors in measuring, calibration, and evaluation procedure of determining Δh_f or comonomer content
2. Different sample preparation (crystallization condition, annealing, cooling from crystallization etc. For example: the samples of curve 3a are as polymerized, those of 3b have been heated up to 450 K and then cooled down with a rate of 20 K/min; samples corresponding to curve 6I have been quenched, those of 6II and 6III have been slowly cooled from the melt).
3. Molecular weight (this together with the particular crystallization conditions widely effects the crystalline morphology). For some curves (1, 4, 5, and 6) the molecular weight also varies in a systematic way with the comonomer content. Moreover, the distribution of molecular weight may play a certain role.
4. Comonomer statistics (homogeneous and heterogeneous copolymers of same comonomer content may crystallize in a quite different way).

CONCLUSION

Fractions, obtained by cross fractionation of a commercial LLDPE, Stamylex 1048, by dynamic direct extraction and subsequent solution crystallization, are

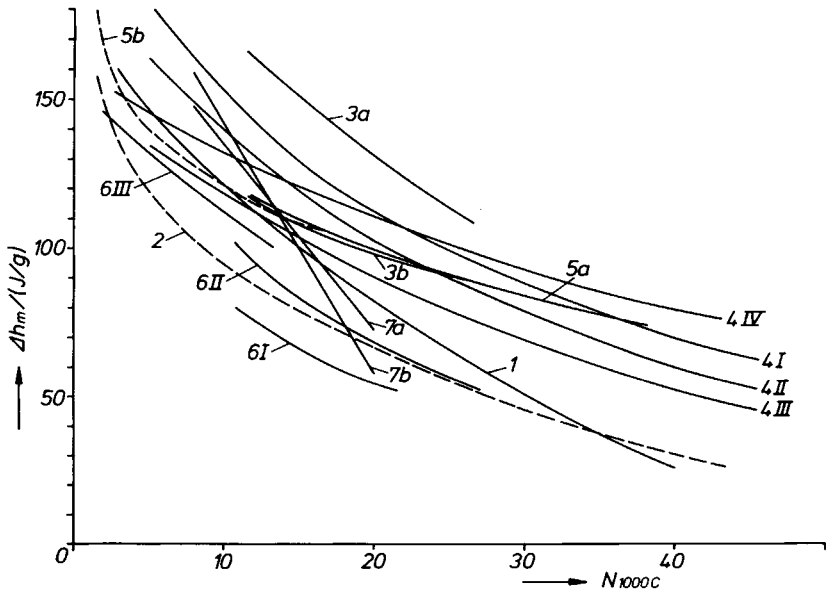

Fig. 13. Relationships between heat of fusion and comonomer content for 1-butene LLDPEs as published in some recent papers. (1, Ref. 8; 2, Ref. 18; 3a, 3b, Ref. 35; 4I–4IV, Ref. 17; 5a, 5b, Ref. 36; 6I–6III, Ref. 37; 7a, 7b, present work.)

characterized by determining molecular weights and comonomer content. A linear dependence of comonomer content on volume fraction of xylene is observed (Eq. (6b)). Also, a linear relationship (Eqs. (7), (8a), and (8b)) between comonomer content and the logarithm of M_η is found, which can be compared to analogous data of other authors. The constants of these empirical equations vary with the investigated 1-butene LLDPEs. The same statement can be made for the linear relationship between comonomer content and temperature of solution crystallization (Eqs. (9) and (10)).

The melting and crystallization behavior of Stamylex 1048 has been discussed and related to similar results, represented in recent articles dealing with 1-butene LLDPEs. Some common tendencies in the relations between comonomer content on the one hand and characteristic temperatures of DTA curves or heats of crystallization and fusion on the other hand are confirmed. But the comparison, moreover, makes obvious that there is a wide spread of the absolute data found for different LLDPEs. This spread may be understood taking into account the particular chemical and morphological structures of the investigated 1-butene LLDPEs as well as the applied measuring conditions.

The authors express their thanks to DSM, The Netherlands, for granting the investigated LLDPE specimen. The help of Dr. J. Kelm, Bundesanstalt für Materialforschung und -prüfung (BAM) is gratefully acknowledged.

References

1. W. F. Maddams and J. Woolmington, *Makromol. Chem.*, **186,** 1665 (1985).
2. S. Bork, *Kunststoffe,* **74,** 474 (1984).
3. V. B. F. Mathot and M. F. J. Pijpers, *Polym. Bull.*, **11,** 297 (1984).
4. V. B. F. Mathot, in *Polycon '84,* 1984, pp. 1–14.
5. V. B. F. Mathot, H. M. Schoeffeleers, A. M. G. Brand, and M. F. J. Pijpers, *Proc. 17 Europhys. Conf. Macromol. Phys., 1985.*
6. P. Shouterden, C. Riekel, M. Koch, G. Groeninckx, and H. Reynaers, *Polym. Bull.*, **13,** 533 (1985).
7. P. Shouterden, G. Groeninckx, B. Van der Heijden, and F. Jansen, *Polymer,* **28,** 2099 (1987).
8. M. F. Mirabella and E. A. Ford, *J. Polym. Sci. Polym. Phys. Ed.*, **25,** 777 (1987).
9. R. Alamo, R. Domszy, and L. Mandelkern, *J. Phys. Chem.*, **88,** 6587 (1984).
10. N. Kuroda, Y. Nishikitani, K. Matzuura, and M. Miyoshi, *Mokromol. Chem.*, **188,** 1897 (1987).
11. W. Holtrup, *Mokromol. Chem.*, **178,** 2335 (1977).
12. D. M. Sadler, *J. Polym. Sci. A-2,* **9,** 779 (1971).
13. G. R. Williamson, B. Wright, and R. N. Haward, *J. Appl. Chem.*, **14,** 131 (1964).
14. L. Wild, T. R. Ryle, D. C. Knobeloch, and I. R. Peat, *J. Polym. Sci. Polym. Phys. Ed.*, **20,** 441 (1982).
15. S. Nakano and Y. Goto, *J. Appl. Polym. Sci.*, **26,** 4217 (1981).
16. G. Constantin, M. Hert, and J.-P. Machon, *Mokromol. Chem.*, **179,** 1581 (1978).
17. K. Kimura, T. Shigemura, and S. Yuasa, *J. Appl. Polym. Sci.*, **29,** 3161 (1984).
18. S. Hosoda, *Polym. J.*, **20,** 383 (1988).
19. T. Usami and S. Takayama, *Polymer J.*, **16,** 731 (1984).
20. H. N. Cheng, *Polym. Bull.*, **16,** 445 (1986).
21. T. Usami, Y. Goto, and S. Takayama, *Macromolecules,* **19,** 2722 (1986).
22. M. Kakugo, Y. Naito, K. Mizunuma, and T. Miyatake, *Macromolecules,* **15,** 1150 (1982).
23. S.-D. Clas, D. C. McFaddin, K. E. Russell, and M. V. Scammell-Bullock, *J. Polym. Sci. Polym. Chem. Ed.*, **25,** 3105 (1987).
24. S.-D. Clas, D. C. McFaddin, and K. E. Russell, *J. Polym. Sci. Polym. Phys. Ed.*, **25,** 1057 (1987).

25. A. Solti, D. O. Hummel, and P. Simak, *Makromol. Chem. Macromol. Symp.*, **5,** 105 (1986).
26. H. Springer, A. Hengse, J. Höhne, A. Schich, and G. Hinrichsen, *Progr. Colloid Polym. Sci.*, **72,** 101 (1986).
27. H. L. Wagner, *J. Phys. Chem. Ref. Data,* **14,** 611 (1985).
28. ASTM Spec. Tech. Publ., D 2238-64, 652 (1964).
29. S. J. Spells, S. J. Organ, A. Keller, and G. Zerbi, *Polymer,* **28,** 697 (1987).
30. G. Ungar and S. J. Organ, *Polym. Commun.*, **28,** 232 (1987).
31. V. Grinshpun, K. F. O'Driscoll, and A. Rudin, *J. Appl. Polym. Sci.*, **29,** 1071 (1984).
32. R. Lew, D. Suwanda, and S. T. Balke, *J. Appl. Polym. Sci.*, **35,** 1049 (1988).
33. L. I. Kulin, N. L. Meijerink, and P. Starck, *Pure and Applied Chem.*, **60,** 1403 (1988).
34. S. Hosoda, K. Kojima, and M. Furuta, *Makromol. Chem.*, **187,** 1501 (1986).
35. D. R. Burfield and N. Kashiwa, *Makromol. Chem.*, **186,** 2657 (1985).
36. S.-D. Clas, R. D. Heyding, D. C. McFaddin, K. E. Russell, M. V. Scammell-Bullock, E. C. Kelusky, and D. St-Cyr, *J. Polym. Sci. Polym. Phys. Ed.*, **26,** 1271 (1988).
37. I. G. Voigt-Martin, R. Alamo, and L. Mandelkern, *J. Polym. Sci. Polym. Phys. Ed.*, **24,** 1283 (1986).

Received February 27, 1989
Accepted August 23, 1989